

Experimental validation of a data-driven step input estimation method for dynamic measurements

Quintana-Carapia, Gustavo; Markovsky, Ivan; Pintelon, Rik; Csurcsia, Péter Zoltán; Verbeke, Dieter Toon

Published in:
IEEE Transactions on Instrumentation and measurement

DOI:
[10.1109/TIM.2019.2951865](https://doi.org/10.1109/TIM.2019.2951865)

Publication date:
2020

Document Version:
Submitted manuscript

[Link to publication](#)

Citation for published version (APA):

Quintana-Carapia, G., Markovsky, I., Pintelon, R., Csurcsia, P. Z., & Verbeke, D. T. (2020). Experimental validation of a data-driven step input estimation method for dynamic measurements. *IEEE Transactions on Instrumentation and measurement*, 69(7), 4843-4851. [8892656]. <https://doi.org/10.1109/TIM.2019.2951865>

General rights

Copyright and moral rights for the publications made accessible in the public portal are retained by the authors and/or other copyright owners and it is a condition of accessing publications that users recognise and abide by the legal requirements associated with these rights.

- Users may download and print one copy of any publication from the public portal for the purpose of private study or research.
- You may not further distribute the material or use it for any profit-making activity or commercial gain
- You may freely distribute the URL identifying the publication in the public portal

Take down policy

If you believe that this document breaches copyright please contact us providing details, and we will remove access to the work immediately and investigate your claim.

Experimental validation of a data-driven step input estimation method for dynamic measurements

Gustavo Quintana Carapia, Ivan Markovsky, Rik Pintelon, *Fellow, IEEE*, Péter Zoltán Csurscia,
and Dieter Verbeke,

Abstract

Simultaneous fast and accurate measurement is still a challenging and active problem in metrology. A sensor is a dynamic system that produces a transient response. For fast measurements, the unknown input needs to be estimated using the sensor transient response. When a model of the sensor exists, standard compensation filter methods can be used to estimate the input. If a model is not available, either an adaptive filter is used or a sensor model is identified before the input estimation. Recently, a signal processing method was proposed to avoid the identification stage and estimate directly the value of a step input from the sensor response. This data-driven step input estimation method requires only the order of the sensor dynamics and the sensor static gain. To validate the data-driven step input estimation method, in this paper, the uncertainty of the input estimate is studied and illustrated on simulation and real-life weighing measurements. The mean squared error of the input estimate was observed near to the Cramér Rao lower bound of the estimation problem.

Index Terms

Metrology, Dynamic measurement, Cramér Rao lower bound, Data-driven signal processing method.

Gustavo Quintana Carapia, Ivan Markovsky and Rik Pintelon are with Vrije Universiteit Brussel, Department of Fundamental Electricity and Instrumentation, 1050, Brussels, Belgium gquintan@vub.be.

Péter Zoltán Csurscia is with the Vrije Universiteit Brussel, Department of Engineering Technology, 1050, Brussels, Belgium, and with Siemens Industry Software NV, RTD Test Division, Interleuvenlaan 68, 3001, Leuven, Belgium. .

Dieter Verbeke is with the Vrije Universiteit Brussel, Department of Engineering Technology, 1050, Brussels, Belgium.

Manuscript received April 19, 2005; revised August 26, 2015.

I. INTRODUCTION

In this paper we consider that a measurement is a dynamic process and a sensor is a dynamic system. The to-be-measured quantity is an unknown input that excites the sensor. The consequent transient response is further processed to estimate quickly the measurand value. The steady-state response of the sensor gives easy access to the measurand value but this approach is mainly exploited for calibration purposes. Calibration of sensor devices from steady state responses are described in [1] for an accelerometer, in [2] for weighing sensor, and in [3] for pressure sensors.

A compensator is an additional dynamic system that acts on the transient response aiming to reduce the sensor transient time. The compensation is motivated by the need of inverting the sensor dynamic effects to recreate the input. The convolution of the compensator impulse response with the sensor transient response yields the input. Therefore, the design of a compensator is based on the sensor model and requires a deconvolution [4]. Examples of input estimation using compensation of the sensor transient response include a recursive estimation of the compensator parameters [5], finite impulse response (FIR) [6], [7] filters and infinite impulse response (IIR) filters [8], [9]. The filters in these works estimate in real-time the unknown input value.

An alternative to the compensation approach is to use digital signal processing methods that are independent of the sensor model. A data-driven method that estimates the unknown level of step inputs by processing the sensor step response was introduced in [10]. This data-driven input estimation method avoids the sensor modeling stage and estimates directly the input. The step input estimation method performance was demonstrated by simulations and experiments on a digital signal processor (DSP) of low cost [11].

To validate the input estimation methods it is necessary to assess the uncertainty associated with their estimates [12], [13]. There are uncertainty propagation studies for model-based compensators such as the FIR and IIR filters for acceleration measurements where the uncertainty is computed in real time [6], [9], [14]. In these works, the uncertainty expression is based on the transfer function or state space representations of the LTI sensor and filter systems. Another way to assess the measurement uncertainty is by observing the results of multiple practical measurements as it is described in [15] for mass and in [16] for temperature sensors. A deconvolution method is implemented to estimate the input waveform in [17] and the uncertainty is obtained from the input estimate covariance. The impact that the signal processing data-driven dynamic error correction has on the uncertainty is investigated in [18]. A statistical analysis of the data-driven step input estimation method [11] was investigated in [19] and the method uncertainty was obtained with a Monte Carlo simulation study.

This paper provides an uncertainty assessment of the data-driven step input estimation method in a real-life application. The measurements were conducted in a weighing system based on a load cell sensor. We observed that even when the whiteness assumptions of the measurement noise are not fulfilled, the step input estimation method still is able to provide a good estimation. We found that the mean squared error of the input estimate is near the Cramér Rao lower bound of the EIV problem. A confidence interval is provided for the input estimate in terms of the number of samples required to satisfy the accuracy specifications of the user.

The organization of the paper is as follows. Section II describes of the step input estimation method and its uncertainty analysis. Section III presents the results obtained from Monte Carlo simulations. Section IV presents the uncertainty results from a practical implementation of the input estimation method. Section V concludes the paper.

II. PRELIMINARIES

The step input estimation method is formulated as a signal processing method where the true value of the input is estimated from the sensor response. The objective of the statistical analysis is to obtain the bias and the covariance of the input estimate.

A. STEP INPUT ESTIMATION METHOD

The step input estimation method estimates the unknown value $\bar{u} \in \mathbb{R}$ of the input $u = \bar{u}s$, where s is the unit step function ($s(t) = 0$ if $t < 0$, and $s(t) = 1$ elsewhere), applied to a bounded-input bounded-output stable linear time-invariant sensor of order n and dc-gain $g \in \mathbb{R}$. The method processes the sequence of step response observations $(\tilde{y}(0), \dots, \tilde{y}(T))$, where $\tilde{y}(t) \in \mathbb{R}$ for $t = 1, \dots, T$, where T is the number of samples, and

$$\tilde{y} = y + \varepsilon. \quad (1)$$

The exact sensor response y is affected by additive Gaussian white measurement noise ε with zero mean and given variance σ_ε^2 . The response of the sensor is a step-invariant discretization of the continuous-time response.

The estimation of the step input level is obtained as the solution of the minimization problem

$$\hat{x} = \underset{x}{\operatorname{argmin}} \left\| \tilde{y} - \tilde{K}x \right\|_2^2 \quad (2)$$

where $\tilde{y} = [\tilde{y}(n+1) \ \dots \ \tilde{y}(T)]^\top$, the first element of the vector $\hat{x} = [\hat{u} \ \hat{\ell}^\top]^\top$ is the estimated step input level, the vector $\hat{\ell}$ is linked to the sensor initial conditions, and the matrix

$$\tilde{K} = \begin{bmatrix} g & \Delta\tilde{y}(1) & \Delta\tilde{y}(2) & \dots & \Delta\tilde{y}(n) \\ g & \Delta\tilde{y}(2) & \Delta\tilde{y}(3) & \dots & \Delta\tilde{y}(n+1) \\ \vdots & \vdots & \vdots & & \vdots \\ g & \Delta\tilde{y}(T-n) & \Delta\tilde{y}(T-n+1) & \dots & \Delta\tilde{y}(T-1) \end{bmatrix} \quad (3)$$

is a Hankel matrix of $(T-n)$ -block rows, constructed from consecutive differences

$$\Delta\tilde{y}(t) = \tilde{y}(t) - \tilde{y}(t-1)$$

of the measured transient response, augmented in the left side with a $(T-n)$ -vector of repeated elements equal to the dc-gain g . The measurement noise ε enters in the matrix \tilde{K}

$$\tilde{K} = K + E, \quad (4)$$

where K is exact data information and E is the measurement noise.

The data-driven step input estimation method builds a system of equations $\tilde{y} \approx \tilde{K}x$. The recursive least-squares (LS) allows for a real-time implementation that solves the systems of equations. However, the structured measurement noise in \tilde{K} is correlated with the measurement noise in \tilde{y} . It is necessary to study the bias and covariance of the LS solution to express the uncertainty of the step input estimate. The uncertainty assessment of the input estimate is crucial for metrology applications.

The data-driven step input estimation method converts the output-error simultaneous model identification and input estimation problem into an errors-in-variables (EIV) input estimation problem. The cost of avoiding the parametric sensor modeling is to deal with a more difficult stochastic framework.

Details of the step input estimation method are described in [11].

B. STATISTICAL ANALYSIS

To obtain the first and second moments of the step input estimate \hat{u} , we need to study the least-squares (LS) solution

$$\hat{x} = \tilde{K}^\dagger \tilde{y} = (\tilde{K}^\top \tilde{K})^{-1} \tilde{K}^\top \tilde{y}, \quad (5)$$

of the overdetermined structured errors-in-variables EIV problem (2), where \tilde{K}^\dagger is the pseudo-inverse matrix of \tilde{K} . Using a second order Taylor series expansion of the inverse matrix we can approximate the LS solution as

$$\hat{x} \approx (I - M + M^2) C^{-1} (K + E)^\top (y + \varepsilon). \quad (6)$$

where

$$C = K^\top K, \quad \text{and} \quad M = C^{-1}(K^\top E + E^\top K + E^\top E). \quad (7)$$

The Taylor series approximation of \hat{x} enables the calculation of the bias and covariance of \hat{x} since the measurement noise ε and E are no more subject to matrix inversion. The bias and the covariance of the estimate \hat{x} is obtained from

$$b(\hat{x}) = \mu - x, \quad (8)$$

$$\text{cov}(\hat{x}) = \mathbb{E} \left\{ (\hat{x} - \mu)(\hat{x} - \mu)^\top \right\}. \quad (9)$$

where $\mu = \mathbb{E}\{\hat{x}\}$, and $x = K^\dagger y$ is the true value. Considering the structure of the EIV problem, the bias and the covariance of the approximation (6) can be expressed as

$$b_p(\hat{x}) \approx C^{-1} \left((K^\top B_1 - B_2)x - (K^\top B_3 - B_4) \right), \quad (10)$$

$$\text{cov}_p(\hat{x}) \approx K^\dagger \left(\sigma_\varepsilon^2 I_{T-n} + C_1 - C_2 - C_2^\top \right) K^{\dagger\top}, \quad (11)$$

where $B_1 = \mathbb{E}\{EK^\dagger E\}$, $B_2 = \mathbb{E}\{E^\top P_\perp E\}$, $B_3 = \mathbb{E}\{EK^\dagger \varepsilon\}$, $B_4 = \mathbb{E}\{E^\top P_\perp \varepsilon\}$, $C_1 = \mathbb{E}\{Exx^\top E^\top\}$, $C_2 = \mathbb{E}\{Ex\varepsilon^\top\}$, and $P_\perp = I - KK^\dagger$.

The bias and covariance given by expressions (10) and (11) depend on the unobservable true values x , K . The measured variable is the sensor step response \tilde{y} , and from its observations we construct \tilde{K} and compute \hat{x} . The substitution of the measured data in the expressions gives an approximation of the bias and covariance estimation. We have then

$$\tilde{b}_p(\hat{x}) \approx \tilde{C}^{-1} \left((\tilde{K}^\top \tilde{B}_1 - \tilde{B}_2)\hat{x} - (\tilde{K}^\top \tilde{B}_3 - \tilde{B}_4) \right), \quad (12)$$

$$\tilde{\text{cov}}_p(\hat{x}) \approx \tilde{K}^\dagger \left(\sigma_\varepsilon^2 I_{T-n} + \tilde{C}_1 - \tilde{C}_2 - \tilde{C}_2^\top \right) \tilde{K}^{\dagger\top}, \quad (13)$$

where $\tilde{B}_1 = \mathbb{E}\{E\tilde{K}^\dagger E\}$, $\tilde{B}_2 = \mathbb{E}\{E^\top \tilde{P}_\perp E\}$, $\tilde{B}_3 = \mathbb{E}\{E\tilde{K}^\dagger \varepsilon\}$, $\tilde{B}_4 = \mathbb{E}\{E^\top \tilde{P}_\perp \varepsilon\}$, $\tilde{C}_1 = \mathbb{E}\{E\hat{x}\hat{x}^\top E^\top\}$, $\tilde{C}_2 = \mathbb{E}\{E\hat{x}\varepsilon^\top\}$, and $\tilde{P}_\perp = I - \tilde{K}\tilde{K}^\dagger$.

The expected values B_1 , B_2 , B_3 , B_4 , C_1 , and C_2 , are described in [19]. The bias and covariance were obtained to extend previous analysis conducted on EIV estimation problems without an imposed structure [20], [21]. It was shown that the bias and variance expressions (12) and (13) are good predictions of the first and second moments of the LS estimate of a Hankel structured EIV problem. The problem formulated by the step input estimation method belongs to this type of structured EIV problems and the derived expressions can be used to find the bias and variance of the input estimate \hat{u} . The bias and variance predictions approximate the empirical bias and variance.

In the rest of this section we describe the Cramér-Rao lower bound (CRLB) of the structured EIV problem. Since the measurement noise is normally distributed, the sensor response observations y are also normally distributed [23]

$$y \sim \mathcal{N}(Kx, \Sigma_x), \quad \text{where} \quad \Sigma_x = \sigma_E^2 \sum_{i=1}^{(T-n)(n+1)} A_i x x^\top A_i^\top + \sigma_\varepsilon^2 I, \quad (14)$$

$A_i \in \mathbb{R}^{(T-n) \times (n+1)}$ are matrices that describe the Hankel structure of K , and σ_E^2 is the variance of the columns of E stacked in a vector. The covariance matrix Σ_x is used to construct the likelihood function of the structured EIV problem

$$l(x) = -\frac{T-n}{2} \ln(2\pi) - \frac{1}{2} \ln |\Sigma_x| - \frac{1}{2} (Kx - y)^\top \Sigma_x^{-1} (Kx - y). \quad (15)$$

The Fisher information matrix is defined as the expected value of the Hessian of the negative likelihood function, where the partial derivatives are evaluated for $\hat{x} = x$. We have

$$Fi(x) = -\mathbb{E} \left\{ \frac{\partial^2 l(\hat{x})}{\partial \hat{x}^2} \right\} = K^\top \Sigma_x^{-1} K - \frac{1}{2} \left(\frac{\partial \Sigma_x}{\partial \hat{x}} \right)^\top (\Sigma_x^{-1} \otimes \Sigma_x^{-1}) \frac{\partial \Sigma_x}{\partial \hat{x}}. \quad (16)$$

The Cramér Rao lower bound of the minimization problem (2) is

$$\text{CRLB}(x) = Fi^{-1}(x). \quad (17)$$

III. SIMULATION RESULTS

A Monte Carlo (MC) simulation was conducted to test the bias and covariance expressions (12) and (13). The MC simulation performed $N_{MC} = 10^6$ runs of the data-driven step input estimation with different realizations of the measurement noise ε . The measurement noise variance was selected to have a signal-to-noise ratio (SNR) in the interval [30 dB, 80 dB]. We are interested in the first element of \hat{x} , which is the input estimate \hat{u} .

The MC simulation was conducted processing $T = 500$ samples of the transient step response \hat{y} generated by a stable LTI sensor of order $n = 5$, with a sampling frequency of $f_s = 4$ kHz. The steady state response of the system is practically reached after 5000 samples because from there on the relative error between the transient response and the steady-state response is smaller than 2%, see Fig. 1.

The difference between the sample mean $\hat{\mu}_1$ of the step input estimates and the true value \bar{u} is the empirical bias b_e .

$$b_e = \frac{1}{N_{MC}} \sum_{i=1}^{N_{MC}} \hat{u}_i - \bar{u} \approx \hat{\mu}_1 - \bar{u}. \quad (18)$$

The sample variance $\hat{\sigma}^2$ of the step input estimates is used to obtain the standard error of the MC simulation σ_e , which decreases with respect to the square root of the number of MC runs N_{MC} .

$$\sigma_e = \frac{\hat{\sigma}}{\sqrt{N_{MC}}}, \quad \text{where} \quad \hat{\sigma}^2 = \frac{1}{N_{MC} - 1} \sum_{i=1}^{N_{MC}} (\hat{u}_i - \hat{\mu}_1)^2. \quad (19)$$

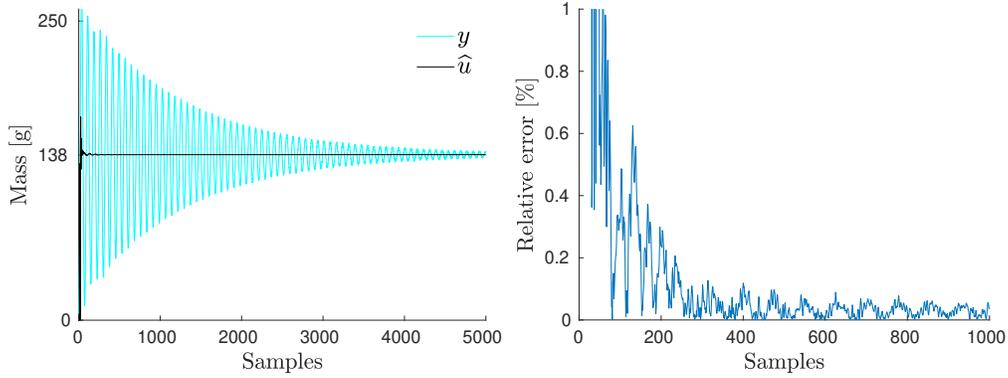


Fig. 1. Left: example of a simulated response \hat{y} and its step input estimation \hat{u} assuming measurement Gaussian noise with 50 dB of SNR. Right: the relative error $|\hat{u} - \bar{u}|/\bar{u}$ is below 1% after 100 samples. We take the estimate at 500 samples because there the relative error is smaller than 0.2%.

In each of the N_{MC} runs we obtain the difference between the LS estimate and the true value, and the prediction of the LS estimate bias and variance from measured data. In the same way we obtained the empirical bias and its associated standard error, we get the sample mean of the bias prediction from observed data \tilde{b}_p and its standard error $\tilde{\sigma}_p$. The predicted bias and variance from exact data are obtained with one evaluation of the expressions (10) and (11).

Fig. 2 shows the sample mean and the standard error of the MC estimates. It can be seen that the empirical biases b_e are proportional to the perturbation noise variance while the standard errors σ_e are proportional to the perturbation noise standard deviation. For SNR below 40 dB there is a difference of a small order of magnitude between the empirical bias b_e and the bias prediction \tilde{b}_p .

The standard errors of the MC estimates σ_e and $\tilde{\sigma}_p$ are smaller than the bias estimates b_e and \tilde{b}_p . The estimates are spread near the sample mean and the uncertainty is smaller than the bias. Therefore, the empirical bias of the MC simulation is meaningful.

The mean squared error (MSE) is defined as

$$\text{MSE}(\hat{u}) = v(\hat{u}) + (b(\hat{u}))^2, \quad (20)$$

where $v(\hat{u})$ is the variance and $b(\hat{u})$ is the bias of the input estimate \hat{u} . The MSE of the step input estimation method is compared to the CRLB of the minimization problem. Fig. 3 shows that the MSE_e , computed from the empirical estimates, and the $\text{MSE}_{\tilde{p}}$, computed from the measured data, have the same proportionality as the CRLB with respect to the measurement noise variance. The difference between the the CRLB and the mean squared errors MSE_e and $\text{MSE}_{\tilde{p}}$ is of small order of magnitude. Therefore, the LS estimation of the structured EIV problem produces results that are comparable to maximum-likelihood

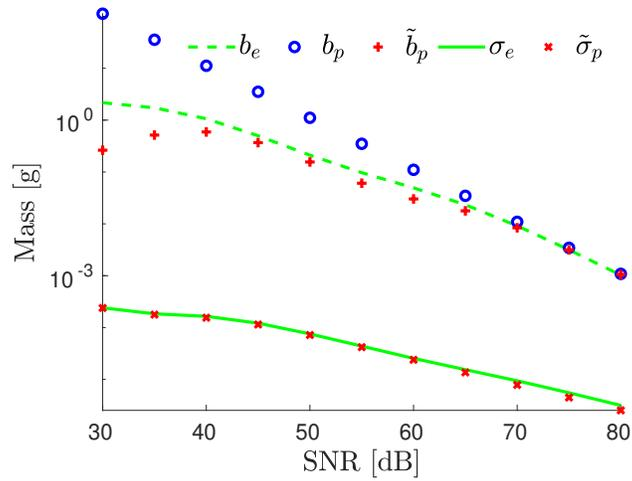


Fig. 2. The results of the Monte Carlo simulation of the step input estimation method are the empirical bias b_e , the predicted bias using exact data b_p , the predicted bias using measured data \tilde{b}_p , the empirical standard error σ_e , and the prediction standard error $\tilde{\sigma}_p$. The estimation biases are proportional to the perturbation variance and the estimation standard errors are proportional to the perturbation standard deviation. Since the standard errors are smaller than the biases, the MC simulation is meaningful.

estimation.

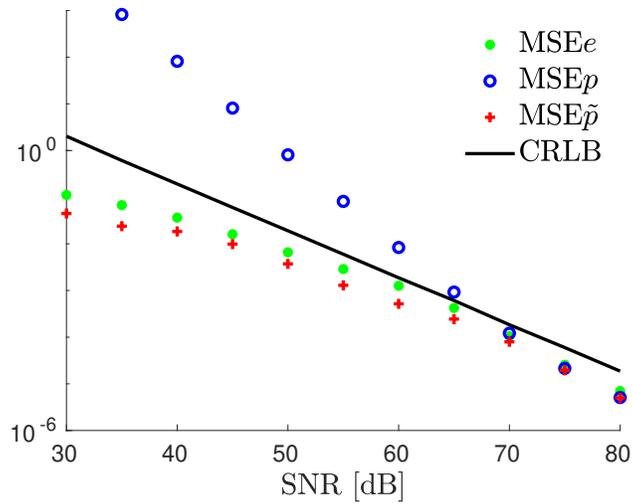


Fig. 3. The MSEs of the LS estimate are close to the Cramér-Rao lower bound of the minimization problem. The MSE of the empirical estimates is represented by MSE_e , and those of the predictions are MSE_p and $MSE_{\tilde{p}}$. The $MSE_{\tilde{p}}$ is smaller than CRLB because of the introduced bias error, but this is not a serious issue since the difference between $MSE_{\tilde{p}}$ and the CRLB is of one order of magnitude for SNR larger or equal than 40 dB.

In order to get more insight into the step input estimation method we conducted another simulation study. The step input estimation method assumes the order n is given in (3). In this simulation, the step

input estimation method processed the step response generated by a $5 - th$ order system using different values of n in the interval from 2 to 100.

The step response is perturbed with Gaussian white noise with SNR values of 30, 40, 50 and 60 dB. For each order n and SNR value, 100 step input estimations are performed from independent noise realizations. Fig. 4 shows the average of the squared biases and the variances, and the MSEs of the input estimate using the first 500 samples. It is evident that the estimation variance and MSE depend on the SNR.

Increasing the order n is equivalent to adding more regressors in the regression problem. It is well known that increasing the order n causes a monotonic decrement of the estimation bias and increment of the variance. This is the asymptotic behavior of the estimation statistical moments with respect to the number of regressors. Nevertheless, the simulation results presented in Fig. 4 show that the variance first increases for small values of n , followed by a decrement and finally after $n \approx 40$ the variances exhibit a slow and steady increment. This apparent contradiction does not prove the invalidity of the estimation method since the results presented correspond to a finite sample size and the asymptotic results cannot be applied. The theoretical explanation of the estimation statistics for finite sample sizes is out of the scope of this paper.

There is a bias-variance tradeoff and the MSEs exhibit local minima with respect to n . The principal contribution to the MSE is the squared bias for the smaller values of n and the variance for the larger values of n . However, the higher orders do not produce overfitting since the MSEs do not grow fast and remain close to the minimum values.

The optimum value of n is not necessarily equal to the order of the generating system and varies for each SNR. According to the plots in Fig. 4, there are orders that provide local minima of the step input estimation MSEs. From the right hand side of Fig. 4, the orders that give the first two MSE minima were identified and those values are listed in Table I. For each SNR, there is a first minimum at a low order and a second minimum at a high order. For SNR of 30 and 40 dB, it is recommended to use the order that gives the first minimum since the MSE at the second minimum is less than one order of magnitude smaller than at the first minimum. Depending on the requirements, the user can choose between the simplicity of an estimation with a low order or an estimation with higher computational complexity and a smaller MSE. In a calibration stage, during the setup of the estimation method, the user can search and set the order that enables the estimation method to provide a required MSE.

TABLE I

ORDERS n THAT PROVIDE LOCAL MINIMA FOR THE MSE OF THE STEP INPUT ESTIMATE. IT IS RECOMMENDED TO USE THE ORDER THAT GIVES THE FIRST MINIMUM WHEN THERE IS A DIFFERENCE OF SMALL ORDER OF MAGNITUDE WITH RESPECT TO THE MSE AT THE SECOND MINIMUM.

SNR [dB]	order at first minimum	order at second minimum
30	11	40
40	7	35
50	4	40
60	3	31

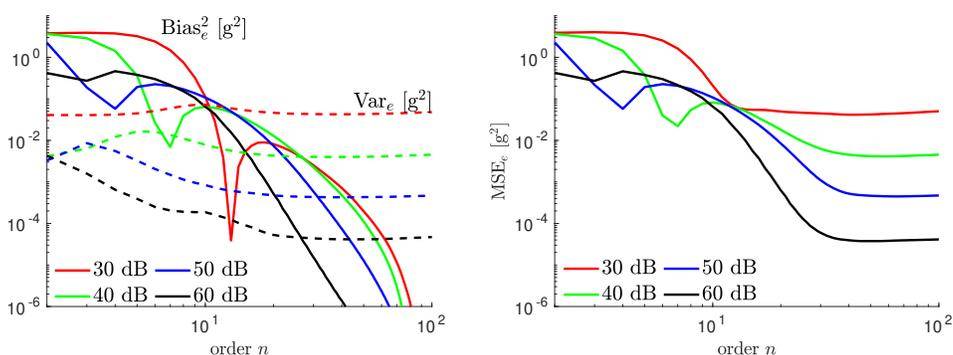


Fig. 4. The simulated step responses of a 5–th order system are processed by the step input estimation method using different orders n and independent noise realizations. The perturbation of the step responses is Gaussian white noise with SNRs of 30, 40, 50, and 60 dB. The square of the empirical bias (solid) and the empirical variance (dashed) are shown on the left hand side and the MSE is shown on the right hand side, for n between 2 and 100. These results suggest that, during the setup of the estimation method, we have to search the order that gives the minimum MSE without increasing unnecessarily the complexity of the estimation method.

IV. PRACTICAL IMPLEMENTATION

An experimental setup was constructed to test the step input estimation method. The implementation is a weighing system that uses a load cell Tedea Huntleigh 1004 [24]. The maximum rating of the load cell is 600 g. An cylindrical aluminium object of 138.32 g of mass was used to excite the load cell. This value was found by calibration using a balance KERN PCB 200-2 that has an uncertainty of 0.01 g. The step input excitation was provided by a magnet that holds and releases a mass from above the load cell. The magnet is located sufficiently far from the load cell to avoid magnetic interference in the sensor response.

A two-stage linear conditioning amplifier performs amplification and filtering of the load cell signal.

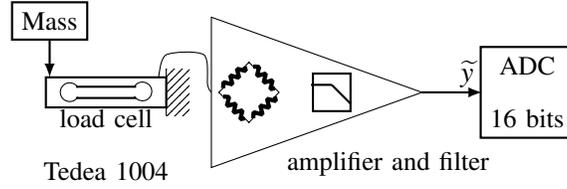


Fig. 5. Diagram of the load cell and the conditioning amplifier that provide the sensor response.

The first stage is an precision instrumentation amplifier INA114 that has high common mode rejection ratio. The second stage is a third-order low-pass Butterworth filter with cut-off frequency of 100 Hz. The low-pass filter prevents the aliasing noise in the measured transient response. The signal obtained from the conditioning amplifier is considered to be the response of the sensor. The sensor responses to step excitations were sampled with a frequency of $f_s = 4$ kHz, and therefore the Nyquist frequency is 2 kHz. The step responses were collected and stored as datasets for further analysis. The number of samples collected for each step response is $N = 20000$. For practical purposes, we consider that the last 10000 samples correspond to the steady state response.

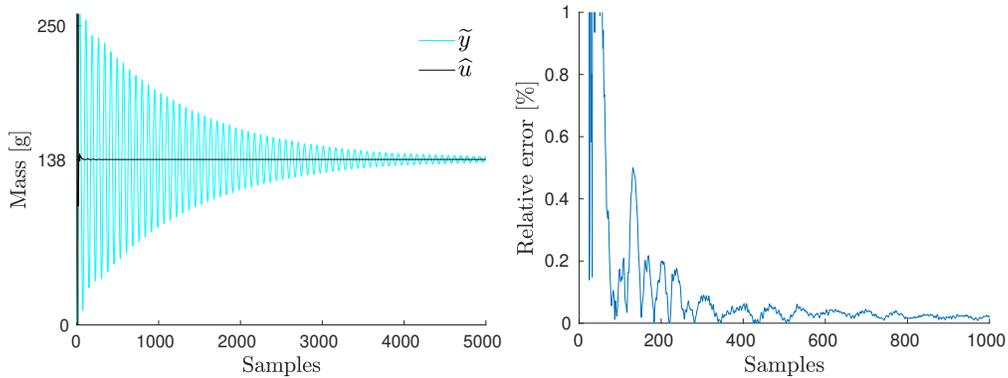


Fig. 6. Left: a typical measured sensor transient response \tilde{y} takes more than 1.25 s (5000 samples, $f_s = 4$ kHz) to converge to the steady state response. Right: the relative error of the input estimate \hat{u} is smaller than 0.2% from 300 samples. We consider that at 500 samples the estimate \hat{u} is small enough to be considered close to its expected value.

The step input estimation method processed 100 measured sensor step responses, assuming the sensor is of 7-th order. Fig. 6 shows a typical measured transient response \tilde{y} and an example of the estimated input \hat{u} .

The empirical bias b_e is the difference between the average of the 100 estimates \hat{u} and the mass calibration value $\bar{u} = 138.32$ g. The bias \tilde{b}_p and variance \tilde{v}_p predictions from the measured data were obtained by processing off-line the 100 measured sensor transient step responses with expressions (12)

and (13). These expressions require the measurement noise variance σ_ε^2 to obtain the bias and variance prediction. One way to estimate the measurement noise variance is computing the variance of each sensor steady state response, see Fig. 7. Later in this section we will explore another way to estimate the measurement noise variance. Computing the noise variance from the steady state response we observed that the SNR of the measured step responses is 55 dB in average.

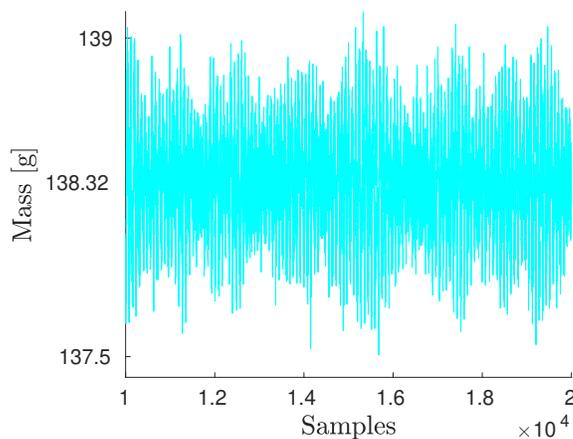


Fig. 7. From the sensor steady-state response an estimation of the measurement noise variance is obtained.

Fig. 8 shows the empirical bias b_e and the standard error σ_e that result after processing the first $T = 500$ samples of the 100 measured step responses y . The standard error is smaller than the bias. As it was observed in the MC simulation, this is the uncertainty of the estimation method. The oscillations observed in the bias are mainly due to the transient response and not to the measurement noise. The measurement noise effects are partially removed since we averaged the 100 transient responses, which is a small number compared with the N_{MC} runs averaged in the simulation section.

It is expected that the empirical bias is large when a small number of samples is processed. The data-driven input estimation method is recursive and it is implemented in real-time. The estimation errors decrease as more data is processed.

The measurement noise is not white since there is evidence of frequency components in the sensor steady state response that are observed as oscillations in Fig 7. To get insight into the properties of the measured sensor response \tilde{y} , a 7-th order model was identified from input-output data assuming that the input is a step of level \bar{u} . A response \hat{y} was simulated from the identified model and the residual $r = \tilde{y} - \hat{y}$ was obtained. We can observe these signals in the frequency domain using the discrete Fourier

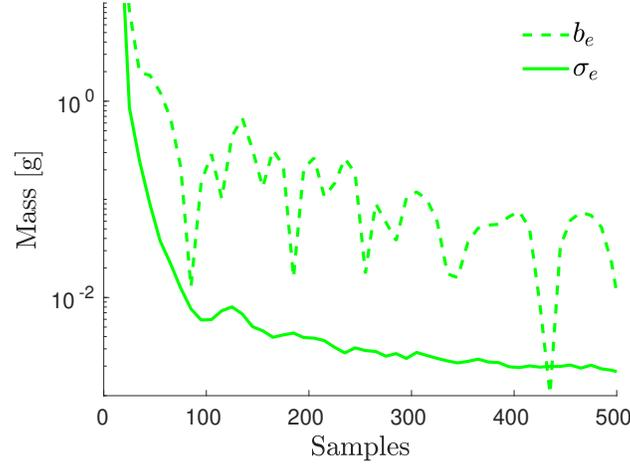


Fig. 8. The results of estimating the step input level after processing 100 measured step responses are the empirical bias b_e and the empirical standard error σ_e . The estimation bias and the estimation standard error decrease as more samples are processed. The estimation bias is affected by the transient effects of the sensor response. The values of b_e and σ_e provide the estimate accuracy and uncertainty for a given sample size.

transform, that for the signal \tilde{y} is defined as

$$\tilde{Y}(l) = \frac{1}{\sqrt{N}} \sum_{k=0}^{N-1} \tilde{y}(k) e^{-j2\pi kl/N} \quad (21)$$

where $l = 1, \dots, N/2$ are the frequency lines and N is the total number of samples. The power spectrum of the signal \tilde{y} is given in decibels by $\tilde{Y}_{\text{dB}}(l) = 20 \log_{10} |\tilde{Y}(l)|$. Figure 9 shows the power spectra of the sensor response Y_{dB} , the simulated response \hat{Y}_{dB} , and the residual R_{dB} . There are frequency components near the main resonance peak in the magnitude spectrum of the residual. The presence of frequency components near the main resonance peak is commonly found in mechanical devices. The vibrations captured from the environment explain the accumulation of energy near the main resonance modes.

Even when the residual r is not white, it provides an alternative way to estimate the measurement noise variance. The average of the residual power spectrum approximates the measurement noise variance as follows

$$\hat{\sigma}_e^2 \approx \frac{2}{N} \sum_{l=1}^{N/2} |R(l)|^2. \quad (22)$$

The dotted line in Figure 9 indicates the $10 \log_{10} (\hat{\sigma}_e^2)$ level of the measurement noise variance estimated from the residual. This level is higher than the mean value of the residual R in the frequencies above 120 Hz.

Using the residual power spectra that correspond to the measured step responses, we obtained the measurement noise variance and the SNR for each experiment. Figure 10 shows the estimated SNRs

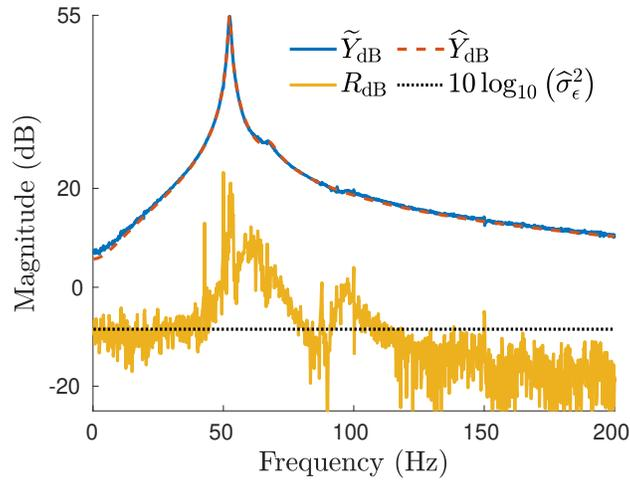


Fig. 9. The power spectra of a measured response \tilde{Y}_{dB} , a simulated response \hat{Y}_{dB} , and the residual R_{dB} is not flat and then the measurement noise is not white. The average of the residual power spectrum provides a conservative estimate of the measurement noise variance $\hat{\sigma}_e^2$, represented with the dotted line.

from the residual power spectra. The SNR mean value is 50 dB. Therefore, we assume that the SNR of the measured transient responses is 50 dB instead of 55 dB, as it was estimated from the steady state response.

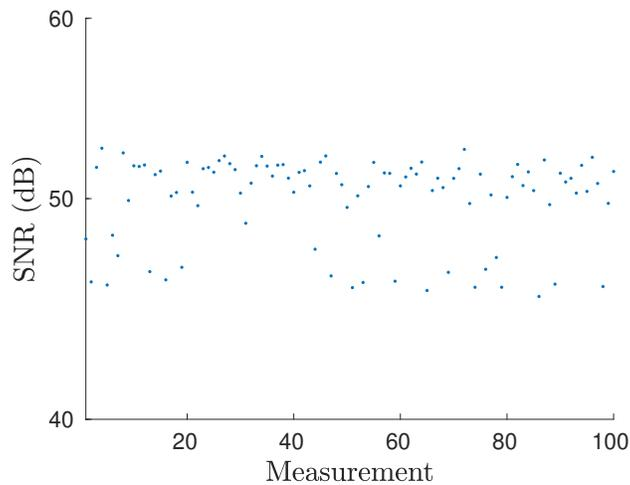


Fig. 10. The mean value of the signal-to-noise ratios estimated from the residual power spectra is 50 dB. We consider that this is the estimated SNR of the measured step responses.

The 5 dB difference provides a conservative bound since the bias and variance computed from 50 dB of SNR are higher than those obtained using the variance estimation from the steady-state response. Fig. 11 shows a comparative of the results obtained with both measurement noise variance estimations after

processing the first $T = 500$ samples of the step response y . Using expression (12), the bias prediction \tilde{b}_{p2} obtained using an SNR of 50 dB approximates more closely the empirical bias than \tilde{b}_{p1} obtained using an SNR of 55dB. In accordance, the standard error of the bias predictions $\tilde{\sigma}_{p2}$ is larger than $\tilde{\sigma}_{p1}$ and is a conservative measure of the input estimation uncertainty. In conclusion, using the noise variance estimated from the residual prevents underestimating the step input estimation uncertainty.

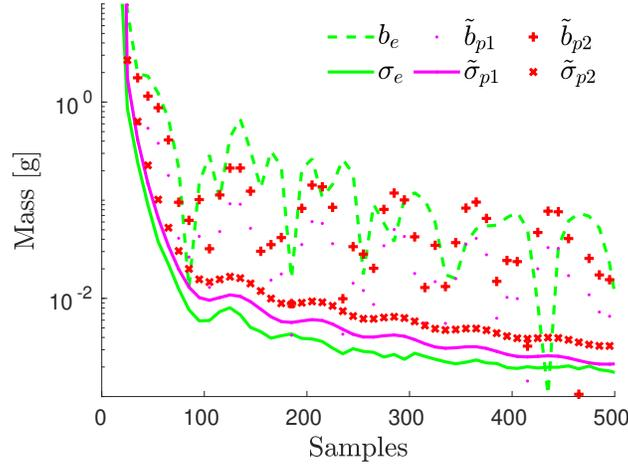


Fig. 11. Comparative view of the bias prediction using two different noise variance estimations. Estimating the variance from the step response residual gives a bias prediction \tilde{b}_{p2} and a standard error $\tilde{\sigma}_{p2}$ that are slightly higher than using the noise variance estimated from the steady state response \tilde{b}_{p1} and $\tilde{\sigma}_{p1}$. The bias prediction \tilde{b}_{p2} approximates better the empirical bias. The standard error $\tilde{\sigma}_{p2}$ provides a conservative value of the input estimation uncertainty.

We investigated another aspect of the step input estimation method performance when processing measured step responses. The step input estimation method requires an assumption of the generating system order in the formulation of the estimation problem (3). The estimation method performance is assessed under different assumptions of the values of n in the interval from 2 to 10. For each value of n , 100 step input estimations are computed from measured transient responses and the empirical MSEs are compared. Fig. 12 shows that, similar to the observations made in the simulation study, the MSEs have two local minima at $n = 7$ and $n = 48$. It is recommended to use $n = 7$ in the estimation method to provide a small estimation MSEs without the higher computational complexity that $n = 48$ implies.

V. CONCLUSION

In this paper we investigated the uncertainty of a data-driven step input estimation method in a real-life application. The step input estimation method is an errors-in-variables problem that is solved with recursive least squares. The statistical analysis of the input estimate provides a tool to assess the

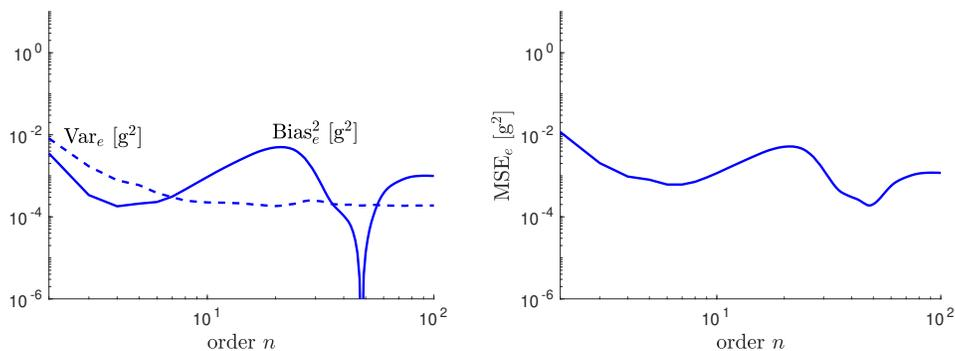


Fig. 12. The hundred measured sensor step responses are processed by the step input estimation method for different values of the order n . The empirical squared bias (solid) and the empirical variance (dashed) are shown on the left and the empirical MSE on the right. The MSE has a local minimum at $n = 7$ and another at $n = 48$. It is recommended to use the estimation method with $n = 7$ because at $n = 48$ the decrement of the MSE is not significant.

uncertainty of the estimate assuming that the measurement noise is Gaussian white noise. In simulation we observed that the mean squared error of the input estimate is close to the theoretical minimum given by the Crámer Rao lower bound. In the practical experiments, the measurement noise is not white. The variance of the sensor steady state response underestimates the measurement noise variance. We introduced a conservative bound of the measurement noise variance so that the first and second moments of the input estimate are more accurately predicted. We can assess the uncertainty of the input estimate with respect to the number of samples processed by the data-driven step input estimation method. The input method is useful in practical applications where the whiteness assumption of the measurement noise is not fulfilled.

ACKNOWLEDGMENT

The research leading to these results has received funding from the European Research Council (ERC) under the European Union's Seventh Framework Programme (FP7/2007–2013) / ERC Grant agreement number 258581 "Structured low-rank approximation: Theory, algorithms, and applications" and Fund for Scientific Research Vlaanderen (FWO) projects G028015N "Decoupling multivariate polynomials in nonlinear system identification" and G090117N "Block-oriented nonlinear identification using Volterra series"; and Fonds de la Recherche Scientifique (FNRS) – FWO Vlaanderen under Excellence of Science (EOS) Project no 30468160 "Structured low-rank matrix / tensor approximation: numerical optimization-based algorithms and applications"; and the Flemish Government (Methusalem award METH1), and

VLAIO Innovation Mandate project number HBC.2016.0235. Dieter Verbeke is funded by a PhD grant from the Research Foundation Flanders.

REFERENCES

- [1] A. Link, A. Täubner, W. Wabinski, T. Bruns, and C. Elster, “Modelling accelerometers for transient signals using calibration measurements upon sinusoidal excitation,” *Measurement*, vol. 40, no. 9–10, pp. 928–935, 2007.
- [2] B. Ando, S. Baglio, and G. L’Episcopo, “A Low-Cost, Disposable, and Contactless Resonant Mass Sensor,” *IEEE Transactions on Instrumentation and Measurement*, vol. 62, no. 1, pp. 246–252, 2013.
- [3] C. Matthews, F. Pennecchi, S. Eichstädt, A. Malengo, T. Esward, I. Smith, C. Elster, A. Knott, F. Arrhén, and A. Lakka, “Mathematical modelling to support traceable dynamic calibration of pressure sensors,” *Metrologia*, vol. 51, no. 3, p. 326, 2014.
- [4] S. Eichstädt, C. Elster, T. Esward, and J. Hessling, “Deconvolution filters for the analysis of dynamic measurement processes: a tutorial,” *Metrologia*, vol. 47, no. 5, pp. 522–533, 2010.
- [5] W. Shu, “Dynamic weighing under nonzero initial conditions,” *IEEE Transactions on Instrumentation and Measurement*, vol. 42, no. 4, pp. 806–811, 1993.
- [6] C. Elster, A. Link, T. Bruns, “Analysis of dynamic measurements and determination of time-dependent measurement uncertainty using a second-order model,” *Measurements Science and Technology*, vol. 18, no. 12, pp. 3682–3687, 2007.
- [7] M. Niedźwiecki, P. Pietrzak, “High-Precision FIR-Model-Based Dynamic Weighing System,” *IEEE Transactions on Instrumentation and Measurement*, vol. 65, no. 10, pp. 2349–2359, 2016.
- [8] R. Pintelon, Y. Rolain, M. Vanden Bossche, J. Schoukens”, “Towards an ideal data acquisition channel,” *IEEE Transactions on Instrumentation and Measurement*, vol. 39, no. 1, pp. 116–120, 1990.
- [9] C. Elster, A. Link, “Uncertainty evaluation for dynamic measurements modelled by a linear time-invariant system,” *Metrologia*, vol. 45, no. 4, pp. 464–473, 2008.
- [10] I. Markovsky, “Comparison of adaptive and model-free methods for dynamic measurement,” *IEEE Signal Processing Letters*, vol. 22, pp. 1094–1097, 2015.
- [11] I. Markovsky, “An application of system identification in metrology,” *Control Engineering Practice*, vol. 43, pp. 85–93, 2015.
- [12] P. da Silva Hack, C. Schwengber ten Caten, “Measurement Uncertainty: Literature Review and Research Trends,” *IEEE Transactions on Instrumentation and Measurement*, vol. 61, no. 8, pp. 2116–2124, 2012.
- [13] A. Ferrero and S. Salicone, “Measurement uncertainty,” *IEEE Instrumentation Measurement Magazine*, vol. 9, no. 3, pp. 44–51, 2006.
- [14] A. Link and C. Elster, “Uncertainty evaluation for IIR (infinite impulse response) filtering using a state-space approach,” *Measurement Science and Technology*, vol. 20, no. 5, pp. 1–5, 2009.
- [15] P. Pietrzak, M. Meller, and M. Niedźwiecki, “Dynamic mass measurement in checkweighers using a discrete time-variant low-pass filter,” *Mechanical Systems and Signal Processing*, vol. 48, no. 1–2, pp. 67–76, 2014.
- [16] J. Ogorevc, J. Bojkovski, I. Pušnik, and J. Drnovšek, “Dynamic measurements and uncertainty estimation of clinical thermometers using Monte Carlo method,” *Measurement Science and Technology*, vol. 27, no. 9, pp. 1–14, 2016.
- [17] P. D. Hale, A. Dienstfrey, J. C. M. Wang, D. F. Williams, A. Lewandowski, D. A. Keenan, and T. S. Clement, “Traceable Waveform Calibration With a Covariance-Based Uncertainty Analysis,” *IEEE Transactions on Instrumentation and Measurement*, vol. 58, no. 10, pp. 3554–3568, 2009.

- [18] B. Saggin, S. Debei, and M. Zaccariotto, “Dynamic error correction of a thermometer for atmospheric measurements,” *Measurement*, vol. 30, no. 3, pp. 223–230, 2001.
- [19] G. Quintana-Carapia, I. Markovsky, R. Pintelon, P. Zoltán, and D. Verbeke, “Bias and covariance of the least squares estimate of a structured errors-in-variables problem,” *Computational Statistics and Data Analysis*, 2019, under review.
- [20] R. Vaccaro, “A Second-Order Perturbation Expansion for the SVD,” *SIAM J. Matrix Anal. Appl.*, vol. 15, no. 2, pp. 661–671, 1994.
- [21] G. Stewart, “Stochastic Perturbation Theory,” *SIAM Review*, vol. 32, no. 4, pp. 579–610, 1990.
- [22] R. Pintelon and J. Schoukens, *System Identification: A Frequency Domain Approach*, 2nd ed. Piscataway, NJ: IEEE Press, 2012.
- [23] A. Beck and Y. Eldar, “Structured Total Maximum Likelihood: An Alternative to Structured Total Least Squares,” *SIAM Journal on Matrix Analysis and Applications*, vol. 31, no. 5, pp. 2623–2649, 2010.
- [24] Tedeo-Huntleigh, “Aluminum Single-Point Load Cell 1004,” Apr. 2015, <http://docs.vpgtransducers.com/?id=2831>.